

PAPER

Temperature dependence of the electrical and thermal transport in FeCo/Cu/Ni₈₀Fe₂₀ spin valves

To cite this article: Shiwei Chen *et al* 2018 *J. Phys. D: Appl. Phys.* **51** 405302

View the [article online](#) for updates and enhancements.

Related content

- [Topical Review](#)
Sarah M Thompson
- [Future perspectives for spintronic devices](#)
Atsufumi Hirohata and Koki Takanashi
- [Topical Review](#)
J F Gregg, I Petej, E Jouguelet *et al.*



IOP | ebooks™

Bringing you innovative digital publishing with leading voices to create your essential collection of books in STEM research.

Start exploring the collection - download the first chapter of every title for free.

Temperature dependence of the electrical and thermal transport in FeCo/Cu/Ni₈₀Fe₂₀ spin valves

Shiwei Chen¹, Zhaolong Yang, Yalu Zuo, Mingsu Si, Li Xi¹, Huigang Shi, Dezheng Yang¹ and Desheng Xue¹

Key Laboratory for Magnetism and Magnetic Materials of Ministry of Education, Lanzhou University, Lanzhou 730000, People's Republic of China

E-mail: yangdzh@lzu.edu.cn (D Yang) and xueds@lzu.edu.cn (D Xue)

Received 20 March 2018, revised 31 July 2018

Accepted for publication 10 August 2018

Published 29 August 2018



Abstract

Creating spin current under temperature gradient in magnetic devices has resulted in a new emerging field of spin caloritronics, but extraction of material parameters i.e. Seebeck coefficient and interpretation of thermal transport characteristics are still great challenges due to the thermal contact effect, especially in a wide temperature range. Because the heat-driven voltages do not depend on the change of magnetic states in spin valve, this could be used to obtain the accurate temperature difference applied on sample and exclude the thermal contact effect. Based on this calibration, the electrical and thermal spin transport behaviors in the in-plane FeCo/Cu/FeNi spin valve were systematically studied with various temperature. We observed that the Seebeck coefficients of spin valve was negative and spin-dependent Seebeck coefficient was proportional to the asymmetry parameter in a wide temperature range from 100 to 300 K, indicating that the spin-dependent thermal transports are closely related with electrical transports in the in-plane spin valve.

Keywords: spin caloritronics, in-plane spin valve, temperature dependence of electrical transport, temperature dependence of thermal transport

(Some figures may appear in colour only in the online journal)

Introduction

Spin caloritronics is a new emerging research field to exploit the interactions among spin, charge, and heat currents in magnetic structures and devices [1]. Owing to combining the spin degrees of freedom associated to the electric charge and heat current, the transports under charge and heat have received renewed interest and been widely investigated in single ferromagnetic layer [2–5], ferromagnetic metal (F)/nonmagnetic metal (N) multilayers [6–13], spin valves [14–19] and magnetic tunnel junctions (MTJs) [20–25]. Similar to the charge current-driven magnetoresistance (MR) effect [26], the heat-driven thermo-electrical power (TEP) also depends on the magnetic states, indicating a spin-dependent Seebeck coefficient. For charge

current-driven magnetic devices, the sign and amplitude of MR are controlled by the spin-dependent asymmetry parameter $\alpha = \rho^\uparrow/\rho^\downarrow$, which reflects the spin-dependent scattering in ferromagnetic layer for spin-up (\uparrow) and spin-down (\downarrow), where ρ is the resistivity [27]. Similarly, in heat-driven magnetic devices, the sign and amplitude of TEP are controlled by the difference of the spin-dependent Seebeck coefficient $S_S = S^\uparrow - S^\downarrow$, where S is the Seebeck coefficient in ferromagnetic layer [28]. For example, for Ni₈₀Fe₂₀ the values of α and S_S at room temperature are 0.40 and $-4.5 \mu\text{V K}^{-1}$, respectively. In case of Co, the values are 0.35 and $-1.8 \mu\text{V K}^{-1}$, respectively [18, 19]. However, the temperature dependent relationships between the spin-dependent electrical and thermal transport for different MR systems are still under debate.

Experiments and theories have shown that the different relationships between the spin-dependent electrical and

¹ Author to whom any correspondence should be addressed.

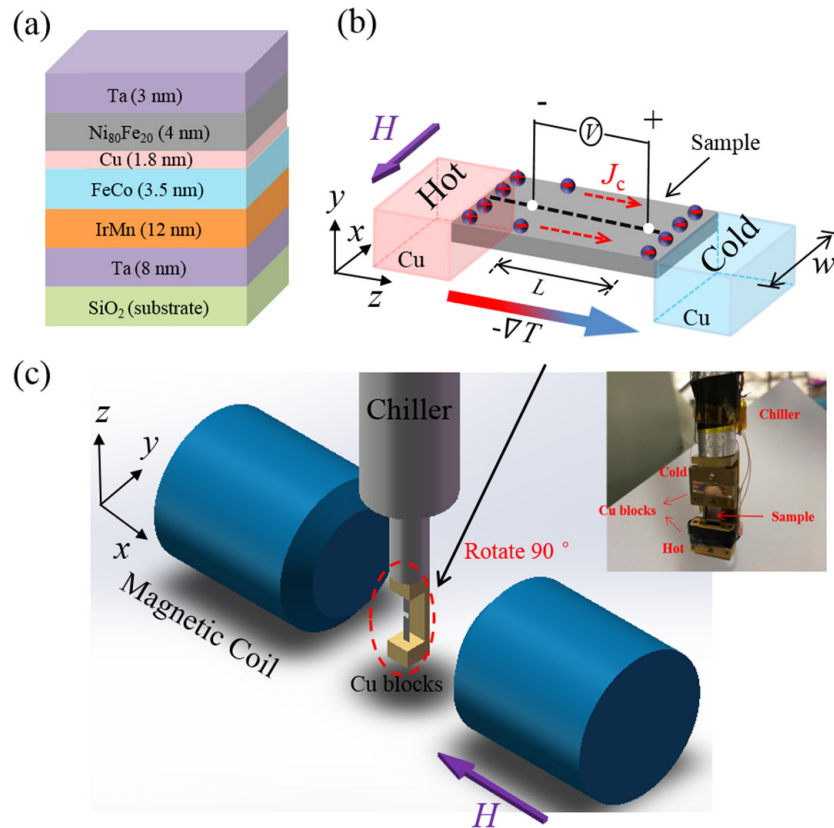


Figure 1. (a) A schematic of a $\text{Ir}_{22}\text{Mn}_{78}/\text{FeCo}/\text{Cu}/\text{Ni}_{80}\text{Fe}_{20}$ multilayer. (b) The magnetothermoelectrical power V is generated under the temperature gradient ∇T . The sample was mounted between two copper blocks, which can provide a stable temperature difference. (c) A schematic experimental device for measuring the magnetothermoelectrical power. The sample holder in figure (b) was rotated in order to show the connection with the chiller in figure (c). The inset of figure (c) is the actual image of the measurement.

thermal transport for the different MR systems. Shi *et al* found that the spin-dependent thermal transports are closely related with electrical transports in current-in-plane (CIP) Co/Cu magnetic multilayers [10]. The Seebeck coefficients obeyed the linear relations with the conductance, when magnetization state in neighboring ferromagnetic layer is gradually changed by external magnetic field. The linear relationship was also valid in $\text{Ni}_{81}\text{Fe}_{19}/\text{Cu}$, Co/CuNi and Fe/Cr multilayers, as well as granular MR systems, which can be considered as a general property [7–11]. The other interesting experiments are based on the non-local thermal spin injection in spin valve [14, 15]. A heat current through the ferromagnetic layer was spin polarized, creating a spin heat accumulation at the interface between F/N by the spin-heat coupling, thus affecting the TEP for parallel (P) or antiparallel (AP) magnetic state of spin valve. According to the modified Fert-Valet spin diffusion equation [29], the spin-dependent Seebeck coefficient was extracted by using a 3D finite-element model [18, 19]. Due to the existence of the spin accumulation at the interface, the relationship of the spin-dependent electrical and thermal transports is complicated. Moreover, experiments and theories both show that TEP and MR effects in MTJs depends on different features of the density of state (DOS) of the ferromagnet layer [22, 23]. The amplitudes of the TEP and MR effects are

not directly linked. However, when the device size is shrunk to nanometer scale, it is still a challenge to determine temperature difference ΔT across thin layers and their interfaces for the extraction of Seebeck coefficient. If the interface temperature difference is not properly taken into account, it could lead to 20 times over-estimation of the Seebeck coefficient in MTJs [24, 25]. Compared with GMR and MTJs with current perpendicular plane (CPP) geometry, the CIP geometry has a clear advantage due to the extended geometry and no interfaces are involved in the relevant direction.

In this work, we report the temperature dependent relationships between the spin-dependent electrical and thermal transport in spin valve with CIP geometry. During the transitions between P and AP magnetic states of spin valve, the changes of TEP are independent of the contact effects. Thus, this allows for an extraction of the temperature gradient to avoid the contact effect. By using the Mott formula, we further abstracted the temperature dependence of the electrical and thermal spin transports coefficients in spin valves. In a wide temperature range from 100 to 300 K, the spin-dependent Seebeck coefficient is proportional to the asymmetry parameter. This validates that the spin-dependent thermal and electrical transports in in-plane spin valve are both dominated by the interface scattering.

Experiments

The spin-valves of glass/Ta (8 nm)/Ir₂₂Mn₇₈ (12 nm)/FeCo (3.5 nm)/Cu (1.8 nm)/Ni₈₀Fe₂₀ (4 nm)/Ta (3 nm) were fabricated by a magnetron sputtering system. The base pressure was 2×10^{-5} Pa and the argon pressure was 0.33 Pa during deposition. During the sputtering a pair of permanent magnets (~200 Oe) is applied to induce a uniaxial anisotropy and exchange bias. The exchange bias field (H_{ex}) at room temperature is about 370 Oe, then gradually increases with decreasing temperature. Figure 1(a) displays a schematic of the sample layout. The width (w) of spin-valve sample is cut into 3 mm. The thermal and electrical transport characteristics of spin valves were measured using standard four-point probe method. Two contacts are fixed to measure the voltage difference with a distance $L = 4$ mm by silver paste. The thermal (electrical) current and magnetic field are perpendicular to each other and both parallel to the film plane, as shown in figure 1(b). To provide the appropriate temperature difference ΔT , the sample was suspended between a pair of Cu blocks. The two Cu blocks can be considered as the heat reservoirs with different temperature, providing a uniform temperature gradient. One Cu block was connected to chiller with temperature T , and the other Cu block was heated by the inside heater to keep its temperature $T + \Delta T$, as shown in figure 1(c). The sample temperatures were monitored and controlled by LakeShore cernox thermometers. We set the temperature at the cold side as the measurement temperature T , and varies the ΔT from 5 to 35 K. When the temperature T and $T + \Delta T$ become stable due to the system PID control, we measured the MTP of spin valve as a function of applied magnetic field. The Seebeck coefficients were extracted by the linear fitting the MTP values dependence of different ΔT . The standard deviation of linear fit is considered as the error values of the Seebeck coefficients. The whole measurements were carried out in the vacuum environment with pressure below 0.1 Pa.

Results and discussion

Spin valve has become a milestone in spintronics [30]. It is consisted with free layer/spacer/pinned layer sandwich structure. When the magnetizations of two ferromagnetic layers are P (AP), the resistivity is high (low). Figure 2(a) shows a typical curve of resistance versus magnetic field in spin valve. Owing to the exchange bias effect, the wide plateau with high resistance in the curves hints the antiparallel alignment of the magnetizations for Ni₈₀Fe₂₀ and FeCo layers [30]. This wide antiparallel alignment of the magnetization is obtained by exchange bias effect in a wide magnetic field. Figure 2(b) shows the TEP of the spin valve as a function of applied magnetic field for different temperature gradient. The characteristic switching clearly shows that Seebeck voltage generated by temperature gradient depends on the relative orientation of the two magnetizations in the spin valve. In comparison with the current-driven magnetoresistance (MR) curve, the heat-driven magneto-thermopower (MTP) curve presents the opposite behavior: the value

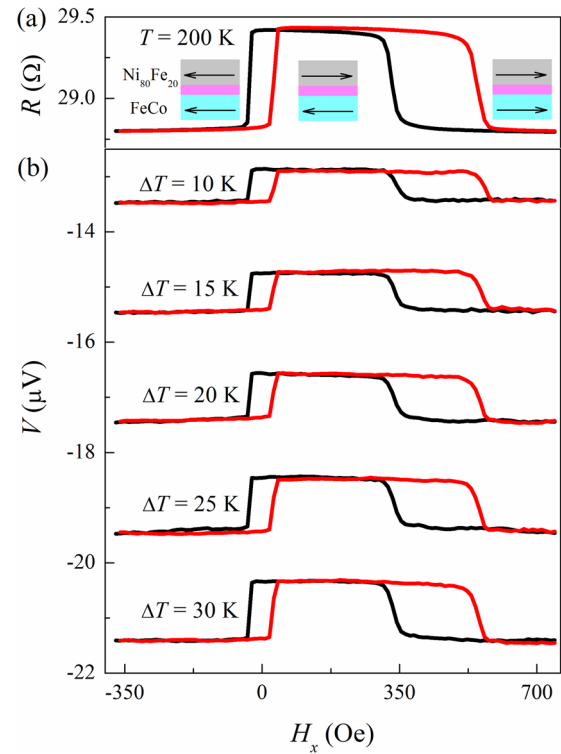


Figure 2. (a) Resistance at current $I = 1$ mA and (b) thermoelectric powers at elevated temperature gradient as a function of magnetic field at 200 K for the Ir₂₂Mn₇₈/FeCo/Cu/Ni₈₀Fe₂₀ spin valve device. The red color presents the forward magnetic field sweeping from -350 (Oe) to 700 (Oe), and the black color presents the backward magnetic field sweeping from 700 (Oe) to -350 (Oe).

of Seebeck is negative, and the absolute value of Seebeck voltage for antiparallel configurations is smaller than the parallel state. It is very important and necessary to compare the S and $\Delta S = S_P - S_{AP}$ for different GMR systems. According to the Mott theory, S is a higher-order transport quantity and can be expressed through the derivative of the conductivity with respect to energy. This means that S and ΔS are closely related with the electronic band structures [13]. For example, for the Co/Cu multilayer the majority density of state (DOS) does not change in the vicinity of the Fermi level. The conductivity change is mainly determined by the change in the electron velocity at the Fermi level. Due to the affection of hybridization between sp and d electrons, increasing the electron energy results in increasing the electron velocity, thus yields both negative signs of S and ΔS . Owing to the similar mechanism, both negative signs of S and ΔS are also observed in other Co/Cu multilayers [7–11], Co–Ni/Cu multilayers [12], Ni₈₁Fe₁₉/Cu/Co spin-valve [17–19], CoFe/Cu/CoFe spin valve [31] and FeNi/Cu/FeNi spin valve [16]. However, contrary to the Co/Cu system, the conductivity of Fe/Cr system is dominated by the minority spins, where the DOS at the Fermi level exhibits a pronounced valley. Increasing electron energy results in moving away from the valley to the region with less-dispersive bands, thus yields both positive signs of S and ΔS [13].

The opposite behaviors for electrical and thermal transports in spin valve can also be simply understood by the two parallel spin channels. For parallel and antiparallel state in

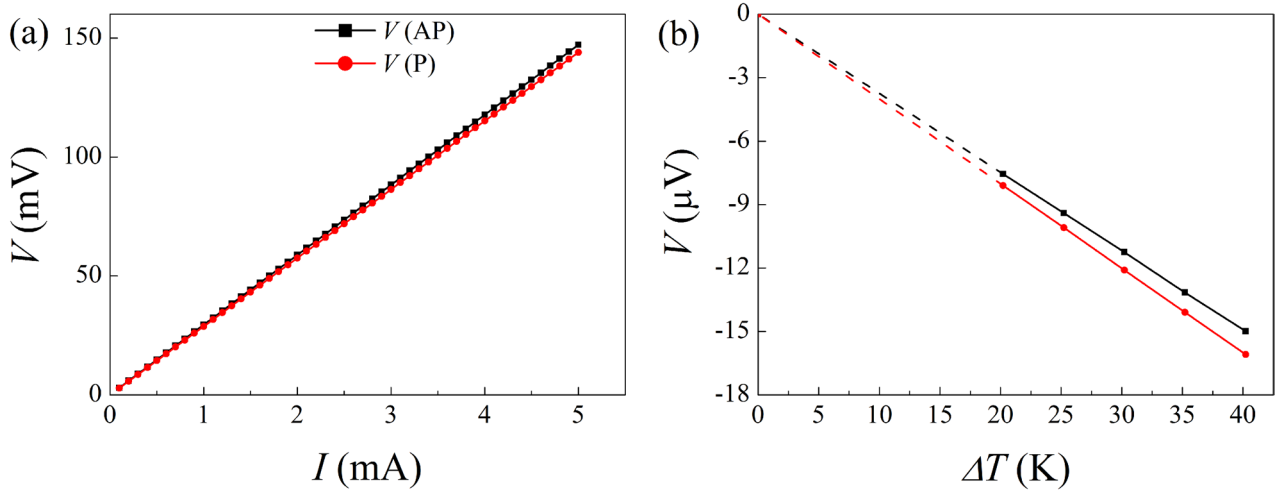


Figure 3. (a) The dependences of voltage on current and (b) thermoelectric power on temperature difference in parallel and antiparallel state at 200K. The I - V and $V - \Delta T$ curves are both linear.

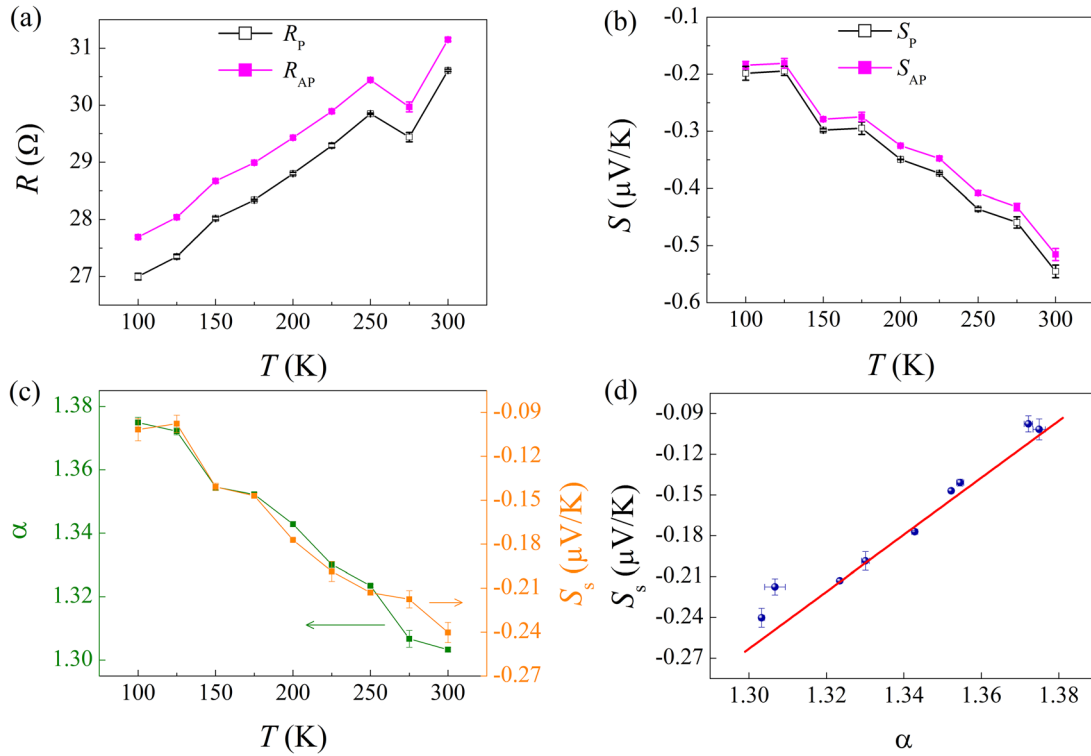


Figure 4. Temperature dependence of (a) the resistance R and (b) the Seebeck coefficient S for parallel and antiparallel magnetic states. (c) The asymmetry parameter α and the difference of spin-dependent Seebeck coefficient S_s as a function of temperature. (d) The difference of spin-dependent Seebeck coefficient S_s has a linear relationship with asymmetry parameter α .

spin valve, this leads to current-driven magnetoresistance and heat-driven magneto-thermopower [7, 10]

$$MR = \frac{\rho_{AP} - \rho_P}{\rho_{AP}} = \left(\frac{\rho^\uparrow - \rho^\downarrow}{\rho^\uparrow + \rho^\downarrow} \right)^2 = \left(\frac{\alpha - 1}{\alpha + 1} \right)^2 \quad (1)$$

and

$$MTP = \frac{S_{AP} - S_P}{S_{AP}} = \frac{(S^\uparrow - S^\downarrow)(\rho^\uparrow - \rho^\downarrow)}{\rho^\uparrow S^\uparrow + \rho^\downarrow S^\downarrow}, \quad (2)$$

where ρ_{AP} and ρ_P (S_{AP} and S_P) are the resistivity (Seebeck coefficient) of spin valve on parallel and antiparallel magnetic

states, respectively. The opposite behavior of MTP indicates that the Seebeck coefficient of spin-up electrons for $Ni_{80}Fe_{20}$ and FeCo layer is more negative than that of the spin-down electrons.

In figure 3(a), the current-driven voltages in P and AP states both linearly increase with the applied charge current, indicating a good ohmic contact. The intercepts for P and AP states are both zero when $I = 0$. In figure 3(b), the heat-driven voltages $V_{P(AP)}$ in P(AP) state also linearly increases with the applied ΔT , which is in agreement with typically measurements of MTP performed on Ferromagnetic/non-magnetic multilayer structures [6–19]. It should be noted that the curves

of $V_{P(AP)}$ as a function of ΔT are shifted to the origin point, according to following two assertions. Because the change of Seebeck voltage in spin valve is induced by switching of magnetizations, independent with the contact effect, we could assert that ΔT should be zero at the point $V_P = V_{AP}$. Moreover, $V_P^0 = V_{AP}^0 \neq 0$ indicates an additional TEP caused by the temperature gradient within the circuitry of voltage meter itself. So it is reasonable to assert that for $\Delta T = 0$, $V_P^0 = V_{AP}^0 = 0$. After this calibration, we could obtain $S_P = -0.54 \mu\text{V K}^{-1}$ and $S_{AP} = -0.51 \mu\text{V K}^{-1}$ at 300K. Analogue to the two-band model in parallel, the Seebeck coefficient in in-plane direction of a multilayer can be also estimated by weighting the Seebeck coefficient S by the corresponding conductance of each layer. The estimated Seebeck coefficient of our spin-valve is $-3.9 \mu\text{V K}^{-1}$. Considering the contact material we used is Al, that $S_{Al} = -1.7 \mu\text{V K}^{-1}$, the Seebeck coefficient of spin valve we obtained is about $-2.2 \mu\text{V K}^{-1}$, which is close to the estimated Seebeck coefficient of spin valve. We also noted that the Seebeck coefficient of our spin valve is consistent with the values of CIP spin valve for Ta/Ru/IrMn/FeCo/Cu/FeCo/Ru system [31].

We systematically studied the spin-dependent electrical and thermal transport as a function of temperature in-plane spin valve. With increasing temperature from 100 to 300 K, R gradually increases from 27.69 to 31.15 Ω , as show in figure 4(a), while S becomes more negative from -0.25 to $-0.55 \mu\text{V K}^{-1}$ in figure 4(b). The small differences between P and AP magnetic states indicate the spin-dependences transports. With increasing temperature, ΔR gradually decreases, while the absolute value of ΔS increases. In metals the diffusion TEP is calculated through the Mott formula [1]

$$S = -\frac{\pi^2 k_B^2 T}{3e} \left(\frac{\partial \ln \sigma(E)}{\partial E} \right)_{E_F}, \quad (3)$$

where e is the elementary charge, k_B is the Boltzmann constant, T is the temperature of sample, and σ is the conductivity of sample. When spin-dependent resistivity was considered, the Seebeck coefficient at parallel and antiparallel magnetic state can be express as

$$\Delta S = S_P - S_{AP} = -\frac{\pi^2 k_B^2 T}{3e} \frac{\alpha'}{\alpha} \left(\frac{\rho_{AP} - \rho_P}{\rho_{AP}} \right)^{1/2}. \quad (4)$$

Here, $\alpha' = \partial \alpha / \partial E$. According to an appropriate assumption in Shi *et al* work, in a simple Born-approximation picture of interfacial scattering, the asymmetry α is dominated by the spin-split DOS in the ferromagnetic material, i.e. $\alpha = g^\downarrow(E_F) / g^\uparrow(E_F)$, where $g^{\uparrow(\downarrow)}(E_F)$ is the final DOS for scattering processes involving up and down spin electrons, thus α' / α can be can be express as following [10]

$$\frac{\alpha'}{\alpha} = \frac{g^{\downarrow'}(E_F)}{g^\downarrow(E_F)} - \frac{g^{\uparrow'}(E_F)}{g^\uparrow(E_F)}. \quad (5)$$

If we consider $S^{\uparrow\downarrow} = (\pi^2 k_B^2 T / 3e) g^{\uparrow\downarrow'} / g^{\uparrow\downarrow}$, thus we can further obtain the following formula

$$\Delta S = S_P - S_{AP} = (S^\uparrow - S^\downarrow) \left(\frac{\rho_{AP} - \rho_P}{\rho_{AP}} \right)^{1/2}. \quad (6)$$

Therefore, substituting the value of R and S on P and AP magnetic states at different temperatures into equations (1) and (6), we can obtain the temperature dependent α and S_S , respectively.

As shown in figure 4(c), with increasing temperature from 100 to 300 K, α linearly decreases from 1.37 to 1.30, while the $-S_S$ linearly increases from 0.10 to 0.24 $\mu\text{V K}^{-1}$. The asymmetry parameter α is consistent with previous experimental results, where for Co/Cu granular systems α are 3.25 and 2.84 for low temperature i.e. 100 K and high temperature i.e. 300 K, respectively [10]. When we set (α , S_S) for different temperatures as points in figure 4(d), we demonstrate that S_S is proportional to α even in the whole temperature range. This result further confirms that the spin-dependent thermal transports are closely related with electrical transports in in-plane spin valve and the relation between spin-dependent thermal transports and electrical transports is independent of temperature. Unlike the spin valves with current perpendicular plane CPP geometry, for spin valves with CIP geometry the spin accumulation and interface temperature difference becomes negligible, thus the spin transport mainly depends on the spin dependence scattering. Therefore, the spin-dependent thermal transports are closely related with electrical transports in CIP-GMR, which provides us a platform to systematically study the relationship between thermal transport and electrical transport, especially in a wide temperature range.

Conclusions

In summary, we have investigated the asymmetry parameter and the spin-dependent Seebeck coefficient in the CIP geometry spin-valve as a function of temperature. For in-plane FeCo/Cu/FeNi spin valve, the value of the Seebeck coefficient and the difference of spin-dependent Seebeck coefficient are both negative. The hybridization between sp and d electrons dominates the resistivity as well as the thermoelectrical power and can be described by the Mott scattering picture. With the varying temperature, the asymmetry parameter and spin-dependent Seebeck coefficient obey a simple liner relationship in the whole temperature range. Our results may provide guidance for further improvements of spin caloritronics.

Acknowledgment

This work is supported by the NSFC of China (Grand Nos. 11774139, 51372107, 11674143), PCSIRT (Grand No. IRT-16R35), and the Program for Science and Technology of Gansu Province (Grand No. 17YF1GA024).

ORCID iDs

Shiwei Chen  <https://orcid.org/0000-0002-8244-1189>

Li Xi  <https://orcid.org/0000-0003-0311-8197>

Dezheng Yang  <https://orcid.org/0000-0001-8527-8519>

References

- [1] Bauer G E, Saitoh E and van Wees B J 2012 *Nat. Mater.* **11** 391
- [2] Pu Y, Johnston-Halperin E, Awschalom D D and Shi J 2006 *Phys. Rev. Lett.* **97** 036601
- [3] Krzysteczko P, Hu X, Liebing N, Sievers S and Schumacher H W 2015 *Phys. Rev. B* **92** 140405
- [4] Madon B, Pham D C, Wegrowe J E, Lacour D, Hehn M, Polewczyk V, Anane A and Cros V 2016 *Phys. Rev. B* **94** 144423
- [5] Uchida K, Takahashi S, Harii K, Ieda J, Koshibae W, Ando K, Maekawa S and Saitoh E 2008 *Nature* **455** 778
- [6] Kimling J, Wilson R B, Rott K, Kimling J, Reiss G and Cahill D G 2015 *Phys. Rev. B* **91** 144405
- [7] Gravier L, Fábíán A, Rudolf A, Cachin A, Wegrowe J E and Ansermet J P 2004 *J. Magn. Magn. Mater.* **271** 153
- [8] Gravier L, Wegrowe J E, Wade T, Fabian A and Ansermet J P 2002 *IEEE Trans. Magn.* **38** 2700
- [9] Baily S A, Salamon M B and Oepts W 2000 *J. Appl. Phys.* **87** 4855
- [10] Shi J, Pettit K, Kita E, Parkin S S P, Nakatani R and Salamon M B 1996 *Phys. Rev. B* **54** 15273
- [11] Hu X K, Krzysteczko P, Liebing N, Serrano-Guisan S, Rott K, Reiss G, Kimling J, Bohnert T, Nielsch K and Schumacher H W 2014 *Appl. Phys. Lett.* **104** 029411
- [12] Böhnert T et al 2014 *Phys. Rev. B* **90** 165416
- [13] Tsybalyk E Y, Pettifor D G, Shi J and Salamon M B 1999 *Phys. Rev. B* **59** 8371
- [14] Slachter A, Bakker F L, Adam J P and van Wees B J 2010 *Nat. Phys.* **6** 879
- [15] Slachter A, Bakker F L and van Wees B J 2011 *Phys. Rev. B* **84** 020412
- [16] Sato H, Miya S, Kobayashi Y, Aoki Y, Yamamoto H and Nakada M 1998 *J. Appl. Phys.* **83** 5927
- [17] Zhang X M, Wan C H, Wu H, Tang P, Yuan Z H, Zhang Q T, Zhang X, Tao B S, Fang C and Han X F 2017 *J. Appl. Phys.* **122** 145105
- [18] Dejene F K, Flipse J, Bauer G E W and van Wees B J 2013 *Nat. Phys.* **9** 636
- [19] Dejene F K, Flipse J and van Wees B J 2012 *Phys. Rev. B* **86** 024436
- [20] Lin W, Hehn M, Chaput L, Negulescu B, Andrieu S, Montaigne F and Mangin S 2012 *Nat. Commun.* **3** 744
- [21] Boehnke A, Walter M, Roschewsky N, Eggebrecht T, Drewello V, Rott K, Munzenberg M, Thomas A and Reiss G 2013 *Rev. Sci. Instrum.* **84** 063905
- [22] Boehnke A et al 2017 *Nat. Commun.* **8** 1626
- [23] Walter M et al 2011 *Nat. Mater.* **10** 742
- [24] Böhnert T, Dutra R, Sommer R L, Paz E, Serrano-Guisan S, Ferreira R and Freitas P P 2017 *Phys. Rev. B* **95** 104441
- [25] Zhang J, Bachman M, Czerner M and Heiliger C 2015 *Phys. Rev. Lett.* **115** 037203
- [26] Wolf S A, Awschalom D D, Buhrman R A, Daughton J M, von Molnar S, Roukes M L, Chtchelkanova A Y and Treger D M 2001 *Science* **294** 1488
- [27] Camley R E and Barnas J 1989 *Phys. Rev. Lett.* **63** 664
- [28] Johnson M and Silsbee R H 1987 *Phys. Rev. B* **35** 4959
- [29] Valet T and Fert A 1993 *Phys. Rev. B* **48** 7099
- [30] Dieny B, Speriosu V S, Parkin S S P, Gurney B A, Wilhoit D R and Mauri D 1991 *Phys. Rev. B* **43** 1297
- [31] Jain S, Lam D D, Bose A, Sharma H, Palkar V R, Tomy C V, Suzuki Y and Tulapurkar A A 2014 *AIP Adv.* **4** 127145